Quantitative Nuclear Evaporation Theory and the Nuclear Potential*†

DAVID B. BEARD AND ALDEN MCLELLAN
University of California, Davis, California
(Received 22 March 1963)

The energy level densities of nucleons in a diffuse nuclear well are calculated using an Eckart-Bethe (Woods-Saxon) potential and shown to be a more sensitive function of energy than the calculated densities of nucleons in a square well having the same volume. The particle spectra of 16-MeV (p,n) reactions and 14-MeV inelastically scattered neutrons are computed including multiple neutron emission. Using realistic values for the effective nucleon mass, the nuclear radius, and the diffuseness parameters we find that the theoretical spectra fit the experimentally observed spectra well within the experimental error. This fit is obtained without the usual experimental parameter fitting of theoretically undetermined constants. Methods of obtaining single-particle emission spectra from experimentally determined particle spectra when multiple-particle emission occurs are discussed. Our work suggests that a careful analysis of precisely measured evaporation spectra will give some information about the dependence of the diffuseness of the nuclear potential on excitation energy.

I. INTRODUCTION

IN the years since Bethe[1] derived a statistically based expression for the energy-level densities in excited nuclei, the theory has undergone extensive development well reviewed by Ericson,[2] LeCouteur,[3] and Bodansky.[4] The simple approximation to the single-particle energy level spacing in a square well has been improved at low excitation energy to take account of nuclear shell structure particularly by Bloch,[5] Rosenzweig,[6] and Ross[7] and a good fit to experimental data obtained. Although the particle spectra from nuclei excited to energies in excess of 10 MeV or so should be interpretable in terms of the simple approximation of particle levels in a square well of known dimensions, experimentally observed particle spectra from highly excited nuclei have frequently not been successfully interpreted in this way. Experimental spectra are not observed to have the energy dependence deduced from a square well whose dimensions are given by elastic scattering measurements.

Part of the difficulty has been that multiple particle emission has sometimes been neglected so that in the semiempirical expression for the expected energy dependence $\exp 2(\alpha E)^{1/2}$ the parameter α which is deduced from experimentally determined spectra usually differs from the theoretical value of the same parameter by an order of magnitude. When multiple particle emission is included so that the excitation energy of the parent nucleus is not treated as constant, we find the theoretical fit to experiment is excellent. However, since the excitation energy of the parent nucleus varies widely for the multiply emitted particles appearing in the spectrum, the experimentally determined "constant" Fermi gas temperature, $(E_{\max}/\alpha)^{1/2}$, is unfortunately not a useful concept in describing the total particle evaporation from nuclei which can successively emit more than one particle. Another difficulty met in comparing experimentally determined particle spectra to a theoretical prediction based on a nuclear square well is that a nuclear square well is not an adequate potential model for energetic nucleons whose wavelengths are less than or comparable to the width of the diffuseness of the actual nuclear potentials. A diffuse nuclear potential will result in greater level densities at high energies of excitation than a square potential well[8] in agreement with the numbers of low-energy particles observed in excess of that predicted by the square potential model.[9]

In Sec. II below we derive an expression for the energy level densities in excited nuclei using an Eckart[10]-Bethe[11] (frequently also referred to as a Woods-Saxon) potential shape, and show the change in predicted level density caused by the diffuseness of nuclear wells. This diffuseness is determined by elastic scattering from nuclei in their ground state. Integral equations are then developed in Sec. III by means of which the many-particle evaporation spectra from highly excited nuclei were numerically computed and compared to the inelastic neutron scattering results at 14 MeV observed by Graves and Rosen,[12] Rosen and Stewart,[13] Ahn and Roberts,[14] and the (p,n) scattering results of Gugelot.[15] Differential equations by which many-particle experimental spectra may be reduced to single-particle spectra and the application of this analysis to determine the

* Assisted by the U. S. Atomic Energy Commission, Contract No. AT(11-1)-34 Proj. 63.
† Part of this work has been reported in D. B. Beard, Bull. Am. Phys. Soc. **4**, 356 (1959) and in Alden McLellan and David B. Beard, *ibid.* **6**, 504 (1961).
[1] H. A. Bethe, Rev. Mod. Phys. **9**, 69 (1937).
[2] T. Ericson, Advan. Phys. **9**, 425 (1960).
[3] K. J. LeCouteur, *Nuclear Reactions*, edited by P. M. Endt and M. Demeur (*North-Holland Publishing Company*, Amsterdam, 1959), Vol. I, Chap. 7, p. 318.
[4] D. Bodansky, Ann. Rev. Nucl. Sci. **12**, 79 (1962).
[5] C. Bloch, Phys. Rev. **93**, 1094 (1954).
[6] N. Rosenzweig, Phys. Rev. **105**, 950 (1957); **108**, 817 (1957).
[7] A. A. Ross, Phys. Rev. **108**, 720 (1957).
[8] D. B. Beard, Phys. Rev. Letters **3**, 432 (1959).
[9] W. J. Knox, A. R. Quinton, and C. E. Anderson, Phys. Rev. **120**, 2120 (1960).
[10] Carl Eckart, Phys. Rev. **35**, 1303 (1930).
[11] H. A. Bethe, Phys. Rev. **47**, 747 (1935).
[12] E. R. Graves and L. Rosen, Phys. Rev. **89**, 343 (1953).
[13] L. Rosen and L. Stewart, Phys. Rev. **107**, 824 (1957).
[14] S. H. Ahn and J. H. Roberts, Phys. Rev. **108**, 110 (1957).
[15] P. C. Gugelot, Phys. Rev. **81**, 51 (1951).

energy dependence of nuclear shape (compressibility of nuclear matter) are described in Sec. IV.

II. ENERGY LEVEL DENSITIES IN AN ECKART-BETHE POTENTIAL

A. The Individual-Particle Level Density

Letting the radial part of the nucleon wave function equal u/r we write the radial wave equation for a nucleon in an Eckart-Bethe (Woods-Saxon) potential with orbital momentum quantum number l as

$$\frac{d^2u_l}{dr^2}+\gamma\left[E+\frac{V_0}{1+\exp\eta(r-R)}-\frac{l(l+1)}{\gamma r^2}\right]u_l=0, \quad (1)$$

where $\gamma=2m/\hbar^2=0.049$ F^{-1} MeV^{-1} and $E=-W$, the binding energy of the nucleon. Since the orbital momentum term is a slowly varying function compared to the nuclear potential over the range of the potential and is less than the potential for the l's of interest, it may be conveniently approximated thereby yielding simpler expressions by setting

$$\frac{1}{r^2}=\frac{\gamma\delta}{1+\exp\eta(r-R)}, \quad (2)$$

where $\delta=1/\gamma R^2$ for the potential range and shape adopted in this work.

Let

$$k=\left\{\gamma\left[\frac{V_0-\delta l(l+1)}{1+\exp\eta(r-R)}-W\right]\right\}^{1/2}.$$

Then the WKB approximation leads to elementary integrals whose solutions are given by

$$n_r=\int_0^{r_1}k\,dr=-\frac{2(\gamma W)^{1/2}}{\eta}\tan^{-1}\left\{\frac{[V_0-\delta l(l+1)]}{W[1+\exp(-\eta R)]}-1\right\}^{1/2}+\frac{\{\gamma[V_0-\delta l(l+1)-W]\}^{1/2}}{\eta}$$
$$\times\log_e\left|\frac{\{[V_0-\delta l(l+1)]/[1+\exp(-\eta R)]-W\}^{1/2}+\{V_0-\delta l(l+1)-\eta W\}^{1/2}}{\{[V_0-\delta l(l+1)]/[1+\exp(-\eta R)]-W\}^{1/2}-\{V_0-\delta l(l+1)-W\}^{1/2}}\right|, \quad (3)$$

where n_r is an integer the radial eigenvalue and r_1 is defined by $k(r_1)=0$. Since $W\ll V_0$ for the energy levels of interest,

$$n_r\sim\pi(\gamma W)^{1/2}/\eta-\{\gamma[V_0-\delta l(l+1)-W]\}^{1/2}\times\eta^{-1}(\eta R+\log_e 4). \quad (4)$$

The second term reduces to the square-well result,

$$n_r=-\{\gamma[V_0-\delta l(l+1)-W]\}^{1/2}R,$$

when $\eta=\infty$, from which

$$W=V_0-\delta l(l+1)-n_r^2/\gamma R^2.$$

The number of states with the same energy is given by

$$N=\sum_{n_r}(2l+1)=\sum_{n_r=0}^{k}[1+4(k^2-n_r^2)]^{1/2}\sim\sum_{l=0}^{k}(2l+1)\sim k^2,$$

where $k^2=(V_0-W)\gamma R^2$.

The usual level density formula for a square well is thus obtained:

$$N\Big/\left(-\frac{\partial W}{\partial k}\right)=N\Big/\left(-\frac{\partial W}{\partial n_r}\right)$$
$$=\tfrac{1}{2}(V_0-W)^{1/2}(\gamma R^2)^{3/2}=\tfrac{1}{2}\epsilon^{1/2}(\gamma R^2)^{3/2},$$

where ϵ is the particle energy measured from the bottom of the well.

Similarly for the diffuse well the single-particle level density may be obtained from Eq. (4) to be

$$\rho\sim-N\frac{\partial n_r}{\partial W}\sim\gamma R^2\epsilon\frac{\partial n_r}{\partial\epsilon}=\frac{\gamma^{3/2}R^3}{2\eta}\epsilon\left(\frac{\pi}{(V_0-\epsilon)^{1/2}}+\frac{\eta R+\log_e 4}{\epsilon^{1/2}}\right)$$
$$\propto\epsilon^{1/2}\left[1+\frac{\pi}{\eta R+\log_e 4}\left(\frac{\epsilon}{V_0-\epsilon}\right)^{1/2}\right]. \quad (5)$$

Note that $\rho\to\infty$ as $W=V_0-\epsilon\to 0$ when η is finite. This is a real and expected result for any potential well which joins smoothly and monotonically to $V=0$ as $r\to\infty$. This result is strictly valid only for $l=0$ because of the centrifugal barrier approximation given in Eq. (2). It is convenient to approximate $[\epsilon/(V_0-\epsilon)]^{1/2}$ by a quadratic series for $1\leq W\leq 8$:

$$[\epsilon/(42-\epsilon)]^{1/2}\sim 2.10+0.088(\epsilon-\epsilon_f)^2,$$

where ϵ_f is the Fermi level, the energy of the highest filled ground state assumed here to be 34 MeV. We thus obtain a simple approximation for the individual-particle-level density in a diffuse well in terms of the individual-particle-level density in a square well (written S.W.):

$$\rho=\text{S.W.}\left\{1+\frac{0.088\pi/(\eta R+\log_e 4)}{1+2.10\pi/(\eta R+\log_e 4)}(\epsilon-\epsilon_f)^2\right\}$$
$$\equiv\text{S.W.}\{1+\lambda(\eta R)(\epsilon-\epsilon_f)^2\}, \quad \epsilon>\epsilon_f. \quad (6)$$

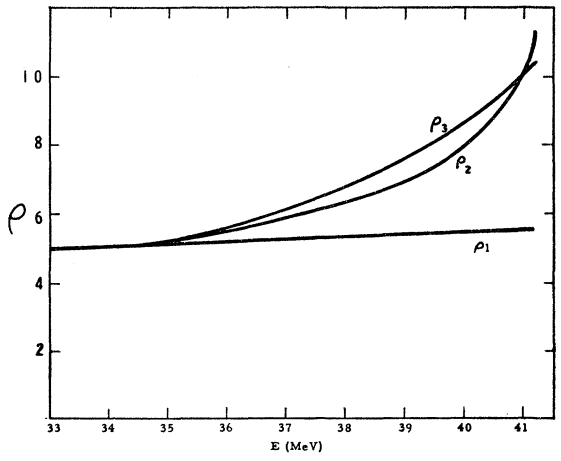

FIG. 1. Different individual-particle level densities for a nucleon in a potential well including a square-well result ρ_1; a diffuse-well result [Eq. (5)] ρ_2; and an approximation to the diffuse-well result [Eq. (6a)] ρ_3. All level density formulas are made equal at the Fermi energy taken to be 34 MeV. ρ is expressed in relative units.

The quantity in braces is the correction factor we have sought to account for the diffuseness of the nuclear potential. If $R=1.3\times100^{1/3}$ F, $\eta=1.45$ F^{-1}, $\lambda(\eta R)$ becomes 0.017, and Eq. (6) becomes

$$\rho=\text{S.W.}\{1+0.017(\epsilon-\epsilon_f)^2\}. \tag{6a}$$

The various formulas including (5) and (6a) for the individual-particle level densities are illustrated in Fig. 1.

B. The Total Nuclear Level Density

Using the Sommerfeld electron theory of metals[1,16,17] we may easily derive the excitation energy as a function of gas temperature for a free nucleon gas in an Eckart-Bethe potential. We assume an individual-particle level density which is the same as the square-well level density for energies below the Fermi energy and is the level density given in Eq. (6) for energies above the Fermi level. That is,

$$\begin{aligned}\rho(\epsilon)&=\frac{2}{3}\frac{N}{\epsilon_f^{3/2}}\epsilon^{1/2}d\epsilon=c\epsilon^{1/2}d\epsilon, && \epsilon<\epsilon_f\\ &=c\epsilon^{1/2}\{1+\lambda(\eta R)(\epsilon-\epsilon_f)^2\}d\epsilon, && \epsilon>\epsilon_f\end{aligned} \tag{7}$$

where N is the number of nucleons in the potential well, V is the volume of the nucleus and the Fermi energy ϵ_f is given by

$$\epsilon_f=\frac{\hbar^2}{8m}\left(\frac{3N}{\pi V}\right)^{2/3}. \tag{8}$$

The total number of nucleons of one kind in the potential is equal to the integral over the particle energy of Eq. (7) times the probability of occupation of the states:

$$N=\int_0^\infty\frac{\rho(\epsilon)d\epsilon}{1+\exp(\epsilon/kT-\xi/kT)}, \tag{9}$$

where ξ is a slowly varying function of temperature chosen to make the integral equal to N. The total energy of all nucleons of one kind in the potential is given by a related integral,

$$U=\int_0^\infty\frac{\epsilon\rho(\epsilon)d\epsilon}{1+\exp(\epsilon/kT-\xi/kT)}. \tag{10}$$

The square-well result is[16,17]

$$U_S=U_0+\left(\frac{\pi}{2}\right)^2\frac{N}{\epsilon_f}(kT)^2-\frac{3}{5}\left(\frac{\pi}{2}\right)^4\frac{N}{\epsilon_f^3}(kT)^4, \tag{11}$$

where ξ has been determined from Eq. (9) and substituted into the result for Eq. (10). To this result must be added the extra diffuse well contribution in Eq. (7):

$$U_D=c\lambda(\eta R)(kT)^{7/2}\int_b^\infty\frac{x^{3/2}(x-b)^2}{1+e^{x-a}}dx,$$

and similarly for N_D, where $x=\lambda/kT$, $a=\xi/kT$, and $b=\epsilon_f/kT$ and $a\sim b\sim34$. By integrating this integral and the one for N_D by parts, we obtain

$$I_m\equiv\int_b^\infty\frac{x^m(x-b)^2}{1+e^{x-a}}dx=\int_b^\infty[mx^{m-1}(x-b)^2+2x^m(x-b)]\times\log_e(1+e^{a-x})dx,$$

where $m=\frac{1}{2}$ for N_D, $\frac{3}{2}$ for U_D. This integral is readily integrated if we expand the logarithm in a series,

$$I_m=\sum_{0=u}^{\infty}\frac{(-1)^{n-1}}{n}e^{n(a-b)}b^{m-1}\left(\frac{2}{nb}+\frac{6m}{(nb)^2}+\cdots\right)\sim1.80b^m+5.68b^{m-1}.$$

We thus obtain

$$\begin{aligned}\xi&\sim\epsilon_f\left[1-\frac{1}{3}\left(\frac{\pi}{2}\right)^2(kT/\epsilon_f)^2-1.80\lambda(\eta R)\epsilon_f^2(kT/\epsilon_f)^3-2.84\lambda(\eta R)\epsilon_f^2(kT/\epsilon_f)^4\right],\\ U&\sim U_0+\left(\frac{\pi}{2}\right)^2\frac{N}{\epsilon_f}(kT)^2-\frac{3}{5}\left(\frac{\pi}{4}\right)^4\times\frac{N}{\epsilon_f^3}(kT)^4+8.5\lambda(\eta R)\frac{N}{\epsilon_f}(kT)^4.\end{aligned} \tag{12}$$

[16] R. H. Fowler and E. A. Guggenheim, *Statistical Thermodynamics* (Cambridge University Press, Cambridge, 1952), Chap. 11, pp. 452–458.

[17] I. N. Snedden and B. F. Toushek, Proc. Cambridge Phil. Soc. 44, 391 (1948).

The first three terms result from the square-well potential. The third term is insignificant and was justifiably neglected in previous derivations of the level density; we shall neglect it in the following. The last term results from the diffuse edge of the well; if $R=1.3\times100^{1/3}$, $\eta=1.45$ F^{-1}, it becomes $0.171(N/\epsilon_f)(kT)^4$ with all energies measured in MeV.

Let

$$\alpha=(\tfrac{1}{2}\pi)^2(N/\epsilon_f),\quad \beta=8.5\lambda(\eta R)(N/\epsilon_f),\quad \tau=kT;$$

then the total nuclear excitation energy becomes

$$Q=U-U_0=\alpha\tau^2+\beta\tau^4. \tag{13}$$

The Helmholz free energy of the gas $F(\tau)$ may then be readily evaluated by use of Eq. (13):

$$F(\tau)=-\tau\int_0^\tau Q(\tau')\frac{d\tau'}{\tau'^2}=-\alpha\tau^2-\tfrac{1}{3}\beta\tau^4, \tag{14}$$

$$e^{-F(\tau)/\tau}=\int_0^\infty \omega(Q)e^{-Q/\tau}dQ, \tag{15}$$

where $\omega(Q)$ is the total nuclear level density we seek. The right-hand side of Eq. (15) is merely the Laplace transform of $\omega(Q)$. Hence, $\omega(Q)$ is given by the inverse Laplace transform[17] of $e^{-F(\tau)/\tau}$:

$$\omega(Q)=\frac{1}{2\pi i}\int_{\gamma-i\infty}^{\gamma+i\infty}\exp\left[QZ+\frac{\alpha}{Z}+\frac{\beta}{3Z^3}\right]dZ,\quad \gamma>0$$

$$\sim\frac{1}{2\pi}\frac{\alpha^{1/4}}{Q^{3/4}}\exp\left\{2(\alpha Q)^{1/2}+\tfrac{1}{3}\beta\left(\frac{Q}{\alpha}\right)^{3/2}\right\}. \tag{16}$$

The method of steepest descent has been used to evaluate this integral and the square root occurring in the evaluation of Z has been expanded in powers of $\beta Q/\alpha$. Snedden and Touschek[17] have shown that the uncertainty introduced by the method of steepest descent is completely negligible.

Equation (16) is the standard nuclear level density formula derived by many authors for a square well with the addition of a factor $\exp(\frac{1}{3}\beta)(Q/\alpha)^{3/2}$. Even for nuclear excitation energies as low as 14 MeV this is a significant factor in determining the emitted particle spectra. It increases rapidly with energy and may become as large as two orders of magnitude for light or medium weight nuclei at excitation energies of 50 MeV.

Figure 2 illustrates the difference in energy dependence of the total nuclear level density for $A=100$ between a square well and a diffuse well as well as the effect of changing α for a square well to simulate a diffuse well. Note that changing α so as to simulate the diffuse well density does not reproduce the slope which is the important quantity.

The parameter β depends on the shape of the nuclear potential. It has been estimated here from elastic scattering data from unexcited nuclei. It would be interesting to learn if it changed with excitation energy as might be expected and thus yield information on the compressibility of the nucleus and the properties of nuclear matter. Experimental interpretation of particle spectra from highly excited nuclei thus may furnish a rare opportunity to determine, however crudely, nuclear properties when the nucleus is not in its ground state. It must first be shown, however, that the level density at lower excitation is well understood and not dependent on additional parameters which must be evaluated by the same experiments.

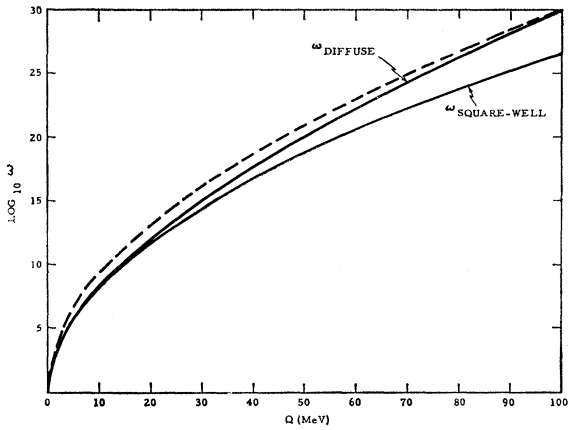

FIG. 2. The total nuclear level density as a function of excitation energy for a square well and a diffuse well with ground-state dimensions. The dashed line is for a square well with adjusted α to match the diffuse-well density at $Q=100$ MeV. The adjusted α is $\frac{1}{2}$ times larger than the calculated α.

III. THEORETICAL QUANTITATIVE PREDICTION OF PARTICLE EMISSION SPECTRA

The emitted particle spectrum $N_1(E)dE$ from a nucleus at original excitation energy E_m is readily obtained from the reciprocity theorem,[18]

$$N_1(E)dE=\text{const}E\sigma_c(E)\omega(Q)dE, \tag{17}$$

where E is the energy of the emitted particle, $\sigma_c(E)$ is the capture cross section of a nucleus at excitation energy $Q=E_m-E$ for a particle of energy E, and $\omega(Q)$ is the level density in the residual nucleus given by Eq. (16).

If $E_m\geqq B_1+B_2+E$, where B_1 and B_2 are the binding energies of the first and possibly second emitted particle, respectively, then a second particle may be emitted which is experimentally indistinguishable from the first particle emitted. (See Feld *et al.*[19] and Tomasini[20] in particular.) In this case the emission spectra of the

[18] J. Blatt and V. F. Weisskopf, *Theoretical Nuclear Physics* (John Wiley & Sons, Inc., New York, 1952).

[19] B. T. Feld, H. Feshbach, M. L. Goldberger, H. Goldstein, and V. F. Weisskopf, Final Report of the Fast Neutron Data Project NYO-636, A.E.C. Document, 1951 (unpublished).

[20] A. Tomasini, Nuovo Cimento **12**, 134 (1954).

second particle is obtained by integrating over the emission spectra of the first emitted particle:

$$N_2(E)=\int_0^{E_m-B_1-B_2-E} N_1(E')N_2(E',E)dE', \quad (18)$$

where $N_2(E',E)$ is the emission spectrum of a particle with energy E from a nucleus with excitation energy (E_m-B_1-E'). Similarly

$$N_3(E)=\int_0^{E_m-B_1-B_2-B_3-E} dE' \times\int_0^{E_m-B_1-B_2-B_3-E-E'} N_1(E'') \times N_2(E'',E')N_3(E'',E',E)dE'', \quad (19)$$

where $N_2(E'',E')$ is the emission spectrum of a particle with energy E' from a nucleus with excitation energy (E_m-B_1-E'') and $N_3(E'',E',E)$ is the emission spectrum of a particle with energy E from a nucleus with excitation energy $(E_m-B_1-B_2-E''-E')$.

Equation (17) is normalized for neutron emission from lowly excited nuclei by requiring that $\int_0^{E_m-B_1} N_1(E)dE=1$ since the probability of emitting one neutron is 100%. However, only a fraction f of the initial excited nuclei are left with enough excitation to emit a second neutron; therefore, Eq. (18) is normalized by requiring that

$$\int_0^{E_m-B_1-B_2} N_2(E)dE=f_2\equiv \int_0^{E_m-B_1-B_2} N_1(E')dE' \Big/ \int_0^{E_m-B_1} N_1(E')dE'. \quad (20)$$

Similarly Eq. (19) is normalized by requiring that

$$\int_0^{E_m-B_1-B_2-B_3} N_3(E)dE=f_3\equiv\int_0^{E_m-B_1-B_2-B_3} N_2(E)dE, \quad (21)$$

in which $N_2(E)$ is assumed already normalized by Eq. (20).

The neutron emission spectrum is peaked so strongly at low excitation energies (~1 MeV) that, in the 14-MeV neutron inelastic scattering analyzed below, $f_2=1$ in every case. The normalization procedure is identical at excitation energies high enough to permit appreciable proton emission, but the expressions are more complicated since competition between two different kinds of particles must be taken into account.

The simplest emission spectrum to consider is neutron evaporation because $\sigma_c(E)$ in Eq. (17) involves only the penetrability through the centrifugal barrier $T_l(E)$ and not the Coulomb barrier as well. Assuming a sticking probability of unity (every particle penetrating the barrier is absorbed), we have

$$\sigma_c(E)=\pi\lambda\!\!\!^{-2}\sum_l(2l+1)T_l(E). \quad (22)$$

By using the values of $T_l(E)$ given by Feld *et al.*,[19] the cross section may be approximated by a power series in $x=0.218RE^{1/2}$, where E is expressed in MeV and R in F:

$A\sim60$, $0.4<x<4.5$:
$\sigma_c(E)/\pi R^2\sim1.35+0.24x^{-1}+0.03x^{-2}+0.02x^{-3}$;

$A\sim115$, $0.4<x<6.0$:
$\sigma_c(E)/\pi R^2\sim1.27+0.105x^{-2}-0.007x^{-3}$;

$A\sim200$, $0.4<x<7.5$:
$\sigma_c(E)/\pi R^2\sim1.10+0.008x-0.014x^{-1}+0.14x^{-3}$.

The cross section asymptotically approaches the geometrical result πR^2 as E and therefore x increases without limit and the geometrical result was used for large x.

The level density parameter α in Eq. (16) is given by

$$\alpha=\frac{\pi^2}{4}\frac{2^{7/3}}{(9\pi)^{2/3}}\frac{mR^2}{\hbar^2}(N^{1/3}+Z^{1/3})=0.0512r_0^2A, \quad (23)$$

where N is the number of neutrons and Z is the number of protons. Snedden and Touschek[17] have shown that an insignificant error is introduced into the calculation if one lets $N=Z=\frac{1}{2}A$, where A is the atomic mass of the nucleus. The parameters r_0, and m, the effective mass of a nucleon while in the nuclear potential, completely determine α. Low-energy scattering experiments establish a value of $1.35f$ for r_0. (A value of 1.5 gives theoretical spectra indistinguishable experimentally from those using a value of 1.35; therefore, we did not bother to recompute spectra where 1.5 had been used inadvertently.) Although the effective nucleon mass has been taken to be one half the free nucleon mass in order to treat nucleon correlations,[1] we used 100% of the free nucleon mass in keeping with our present understanding of nuclear matter.

The essence of the individual-particle model is the assumption that the numerous short-range nucleon-nucleon interactions may be replaced by an effective static potential field,

$$U(x_p)=\sum_i\langle i|V_{pi}|i\rangle,$$

where V represents the nucleon-nucleon potential and the summation is carried out over all the particles in the nucleus. The Pauli exclusion principle causes the potential to be energy-dependent since the interaction between one nucleon and another depends on there being enough shared energy for both particles to be scattered to unfilled states. (The contribution of virtual states being less if energy is not conserved.) Since U may depend quadratically on particle wave number k, as does the kinetic energy, the net result at low energy is for the particle to have an effective mass about half the free

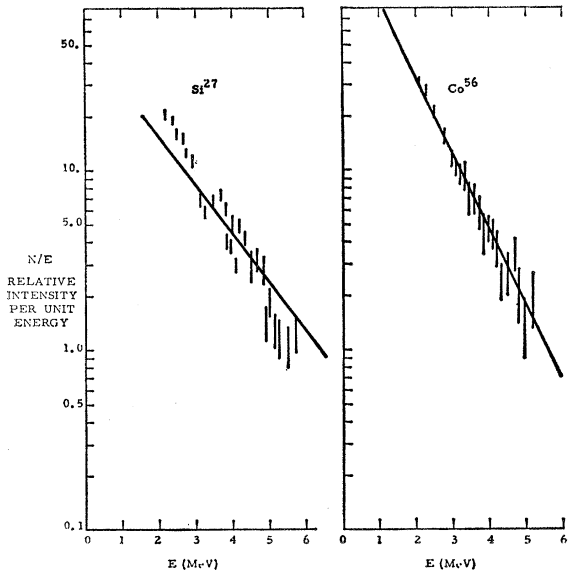

FIG. 3. Neutron spectra resulting from 16-MeV incident protons. Curve on left, theoretical prediction for one emitted neutron from Al^{27} target with nuclear radius $=1.5A^{1/3}$ F. Curve on right, for total of two emitted neutrons from Fe^{56} target with nuclear radius $=1.5A^{1/3}$ F. Experimental points taken from Gugelot (Ref. 15).

nucleon mass.[1,21] At high energy the nucleus becomes black (the exclusion principle is less effective) and the nucleon-nucleon potential becomes more nearly that for free particles. Thus, the effective mass of the nucleon approaches the free nucleon mass. Bethe, Brandon, and Petschek[22] have concluded that the effective nucleon mass for particles with momentum greater than the Fermi momentum is more nearly 9/10 of the free nucleon mass. As can be seen in Fig. 7 an improbable choice of mass lower by a factor of 2 than the free-particle mass is incompatible with the experimental data.

Equation (16) and (22) were substituted into Eqs. (17)–(19) and the integrals were numerically integrated at the Western Data Processing Center for initial excitation energies of $E_m=14$ MeV$+B_1$ in order to obtain a comparison with Graves and Rosen's,[12] Rosen and Stewart's,[13] and Ahn and Roberts'[14] neutron inelastic scattering experiments, and Gugelot's[15] observations of (p,n) scattering at 16 MeV. Neutron binding energies were computed from Baker and Baker's[23] nuclear mass formula. Representative results are plotted in Figs. 3–5, 7 for M equal to the free nucleon mass and $R=r_0A^{1/3}$ for $r_0=1.35$ F and 1.5 F. As can be seen from the figures a satisfactory fit to experiment is obtained at moderate nuclear excitation. Bloch,[5] Rosenzweig,[6] Critchfield and Oleksa,[24] and others have emphasized the level density dependence on nuclear shell configuration at excitation energies of only a few MeV; and therefore, we cannot anticipate a good prediction of the experimental data above emitted particle energies of 4 MeV or so at this excitation energy, particularly for gold which is only three protons removed from a closed shell.

In most applications the labor of numerical integration may be avoided by simple approximations which match the numerically obtained results well within the present theoretical and experimental uncertainties. Let all nucleon energy distributions in the integrand be approximated by neglecting the slowly varying factor $\sigma_c(E)Q^{-3/4}$ and expanding the radical in the exponent. The emission spectrum of the kth emitted particle in the integrand will then be

$$N_k(E_k)dE_k\sim\text{const}\,E_k\left[1-\frac{1}{4T_k}\frac{(\sum_{i=1}^{k}E_i)^2}{E_m-\sum_{i=1}^{k}B_i}\right]\times\exp\left[-\sum_{i=1}^{k}E_i/T_i\right]dE_k, \quad (17a)$$

where B_i is the binding energy of the ith emitted particle and $T_k^2=(E_m-\sum_{i=1}^{k}B_i)/\alpha$. For $E_m-\sum_{i=1}^{k}B_i>20$ MeV the

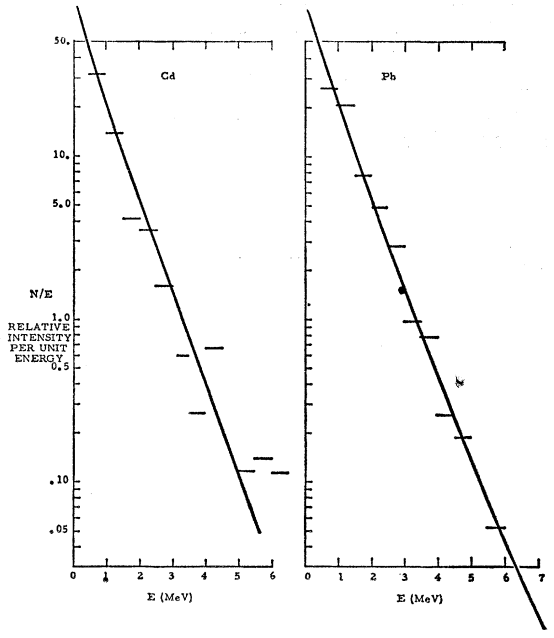

FIG. 4. Neutron spectra resulting from 14-MeV incident neutrons. Curve on left theoretical prediction for total of two emitted neutrons from an isotopic target mixture of Cd^{110} 13%, Cd^{111} 13%, Cd^{112} 24%, Cd^{113} 13%, Cd^{114} 29%, and Cd^{116} 8%with nuclear radius $=1.5A^{1/3}$ F. Curve on right same for isotopic target mixture of Pb^{206} 27%, Pb^{207} 21%, and Pb^{208} 52% with same radius. Experimental points taken from Graves and Rosen (Ref. 12).

[21] H. A. Bethe, Phys. Rev. **103**, 1353 (1956).
[22] H. A. Bethe, B. H. Brandow, and A. G. Petschek, Phys. Rev. **129**, 225 (1963).
[23] G. A. Baker, Sr., and G. A. Baker, Jr., Can. J. Phys. **34**, 423 (1956).
[24] C. Critchfield and S. Oleksa, Phys. Rev. **82**, 243 (1951).

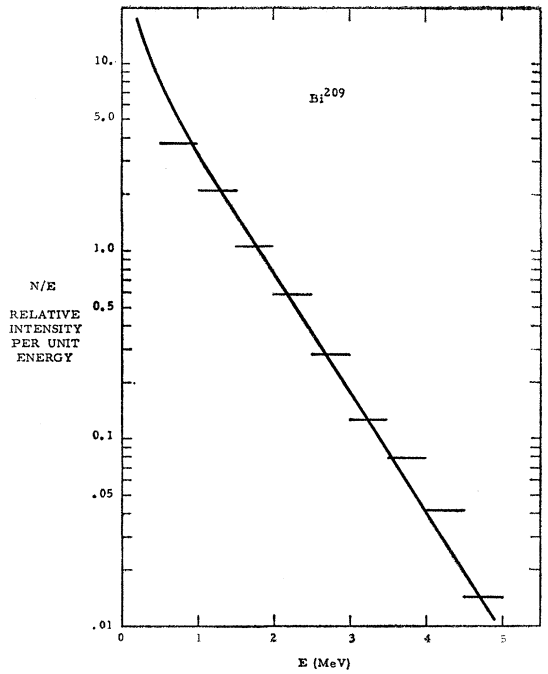

FIG. 5. Neutron spectra resulting from 14-MeV incident neutrons. Solid line is theoretical prediction for total of three emitted neutrons from Bi^{209} target with nuclear radius $=1.35A^{1/3}$ F. Experimental points taken from Rosen and Stewart (Ref. 13).

quadratic energy-dependent factor may be neglected. For the last particle out it is better to leave the energy as part of the temperature which in no way complicates the calculation of the spectrum since this energy is not an integrated variable. Hence, for the contribution of the l'th emitted particle to the total spectrum the approximation becomes

$$N_l(E_l)\sim\text{const}\, E_l\left[1-\frac{1}{4T_l}\frac{(\sum_{i=1}^{l-1}E_i)^2}{Q_l}\right]\times\exp[-\sum_{i=1}^{l-1}E_i/T_l]\exp[2(\alpha Q_l)^{1/2}], \quad (17b)$$

where

$$T_l^2=Q_l/\alpha \quad \text{and} \quad Q_l=E_m-\sum_{i=1}^{l}B_i-E_l.$$

Thus, for the second emitted particle we have considered, an elementary integration (neglecting quadratic terms) yields

$$N_2(E)dE\sim\text{const}\int_0^{Q_2}EE'\exp[-E'(T_1^{-1}+T_2^{-1})]\times\exp[(2\alpha Q_2)^{1/2}]dE'$$
$$\sim\text{const}E\exp[2(\alpha Q_2)^{1/2}]. \quad (18a)$$

In general, when proton competition may be neglected, the total emitted neutron spectrum may be approximated as

$$N(E)dE=E\sum A_j\exp[2(\alpha Q_j)^{1/2}],$$

where the sum is taken over all j for which

$$Q_j=E_m-\sum_{i=1}^{j}B_j-E$$

is positive and

$$A_j=\frac{\alpha f_j}{Q_j+E}\exp\{-2[\alpha(Q_j+E)]^{1/2}\}.$$

The normalization factor f_j is one except for the last emitted neutron.

Each single emission spectrum has the expected concave downward curvature when plotted against E rather than $Q^{1/2}$. The total emission spectra is surprisingly linear except near $E=0$ when normally energy-independent factors such as $\sigma_c(E)$, E^{-1}, and $\exp[(\frac{1}{3}\beta)(Q/\alpha)^{3/2}]$ cause the curve to become concave upward. The linearity of the plot has led to a customary interpretation of the slope of these curves as a reciprocal "temperature" of the nuclear gas. This is not useful since, as Tomasini[20] in particular, has shown, the slope of this curve does not depend in a simple way on the excitation conditions of the initial target nucleus when more than one neutron is emitted. Hence, it is a relatively useless kind of average excitation parameter for the initial and all subsequent emissions. Indeed, this "temperature" might well decrease with excitation energy as more and more particles are emitted. It should also be noted that if the slope of the total emission curve is used to experimentally evaluate α (in an attempt to use the experimental data in this way to fit an expected level density dependence of $\exp[2(\alpha Q)^{1/2}]$, a very different value of α from the one we have calculated is obtained.

The theoretical value of α which results in the markedly different slope of the first emitted neutron spectrum is larger by about an order of magnitude than the α erroneously interpreted in the past by one of the authors (DBB) and others from the slope of the observed multiple emission spectra. Some attempts have been made to explain the difference between theoretical and erroneous "experimental" values of α by an additional contribution from considerations of angular momentum. To be appreciable the moment of inertia must be much smaller by a factor of one or two orders of magnitude than the rigid-body moment of inertia to be expected at these excitation energies on theoretical grounds. As indicated by the figures, angular momentum considerations are not required to account for the experimental spectra.

Fortunately, direct interaction processes were not enough at these energies to complicate the interpreta-

tion. When direct interaction is significant as may be ascertained by angular measurements, the direct interaction (anisotropic scattering) must not only be subtracted out but account must also be taken of the evaporation subsequent to direct interaction from nuclei initially excited to energies much less than the maximum energy resulting from absorption of the incident nucleon. (The isotropic low-energy nucleons resulting from direct interaction have long wavelengths and a short mean free path in the nucleus so that relatively few of them may be expected to contribute to the emission spectrum. Therefore, they are not expected to contribute significantly compared with the results of compound nucleus formation.)

Angular-momentum considerations are not significant for single-nucleon excited nuclei at these energies. The effect of angular momentum on the level density was first considered by Bethe,[1] then later by others including Snedden and Touschek.[17] In rederiving the level density formula to include those states within an energy band Q and $Q+dQ$ *with the quantum number* J, Snedden and Touschek arrive at approximately the same formula as given in Eq. (16) with Q replaced by $Q-\langle J\rangle^2\hbar^2/2I$, where $I=\frac{2}{5}AMR^2$ is the moment of inertia of a solid sphere of mass AM, $A=$atomic weight, $M=$mass of nucleon, and $\langle J\rangle$ is the average value of the angular momentum quantum number in the compound nucleus formed by absorption of the bombarding nucleon. Since each J state has a degeneracy of $2J+1$,

$$\langle J\rangle=\sum_{J=1}^{J=J_{\max}}(2J+1)J\Big/\sum_{J=1}^{J=J_{\max}}2J+1,$$

where $J_{\max}$ is $Rp/\hbar$, R is the radius of the target nucleus, and p the linear momentum of the bombarding nucleon. For large values of $J_{\max}$, $\langle J\rangle\sim\frac{2}{3}J_{\max}$. For 14-MeV neutrons on Ag^{109}, $J_{\max}\approx 6$ and $\langle J\rangle\approx 4$. The effect of angular momentum at this excitation energy is shown in Fig. 6. The angular momentum of the excited and residual nucleus was included in the calculation and as can be seen from Fig. 6 it has negligible effect.

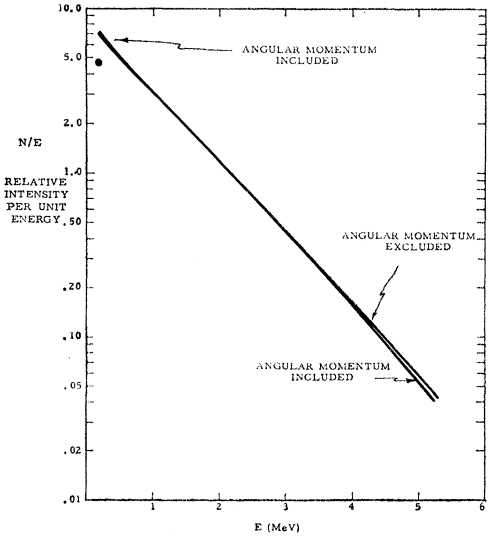

FIG. 6. The effect of including angular momentum in the calculated spectrum from a target of Ag^{109} bombarded by 14-MeV neutrons.

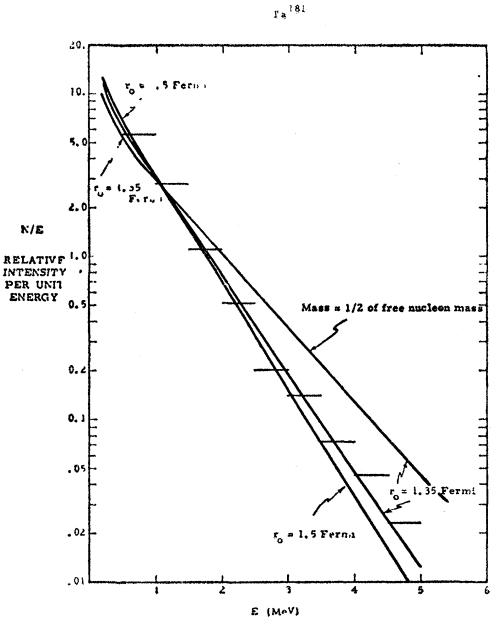

FIG. 7. The effect of varying nucleon mass from 1 to $\frac{1}{2}$ the free nucleon mass and nuclear radius from $1.5A^{1/3}$ to $1.35A^{1/3}$ F in the calculated spectrum from a target of Ta^{181} bombarded by 14-MeV neutrons. Experimental points taken from Rosen and Stewart (Ref. 13).

The relative insensitivity to a choice of r_0 can be seen in Fig. 7 which compares the effect of using $r_0=1.5$ F and $r_0=1.35$ F in the calculation of α as well as the effect of using a nucleon mass half that of the free nucleon mass.

The effect even at these low excitation energies of a diffuse nuclear potential as compared to a square well is illustrated in Fig. 8. This effect is enhanced at higher excitation energies since it depends exponentially on the three-halves power of the excitation energy. The effect is additive so that the total emission spectrum will depart from the square-well spectrum more than the single-particle spectrum illustrated in Fig. 8.

IV. ANALYSIS OF PARTICLE SPECTRA FROM EXCITED NUCLEI

The experimental confirmation at modest excitation energies of the theory presented in the previous section gives one confidence in its formulation. At higher excitation energies, however, further complications may arise since the parameter β may change due to a kind of "thermal expansion" of the potential well. Possible change in nuclear shape with excitation energy has been a source of some controversy in the literature. Proper analysis of the particle spectra (especially charged-

particle spectra) from nuclei at high excitation energy of more than 20 MeV might enable one to determine the change in β with excitation energy. This has the exciting consequence of enabling one to determine the properties of nuclear matter (e.g., compressibility) under otherwise impossibly obtainable conditions.

Nuclear evaporation following absorption of nucleons having an energy of the order of 10–50 MeV will result in an isotropic angular distribution[25] unless energetic heavy incident ions are used for excitation. The contribution of direct-interaction processes may be determined from the angular dependence of the emitted particles. The subsequent emission of particles from nuclei partially excited by direct-interaction processes can then be calculated by the methods of the previous section. This emission which follows direct-interaction processes plus the direct-interaction spectra itself can then be subtracted from the total observed differential cross section in order to obtain the spectrum of multiple emission of protons and neutrons following excitation of the target nuclei to the maximum excitation energy. In evaluating the contribution of direct-interaction processes from nuclei excited by energetic heavy incident ions, the angular dependence introduced by the large angular momentum carried by the incident ion further complicates the interpretation[9,26,27] in that the compound nucleus decay results in a predictable angular dependence of the emitted particles. The interpretation remains straightforward, however, since the angular dependence of the compound nucleus decay may be included by using the results of Ericson and Strutinski[27] and others and sorted out from the direct-interaction angular dependence. To simplify the discussion in the following we will neglect the necessary but straightforward modification of the theory introduced by considerations of angular momentum. We note, however, that the rigid-body moment of inertia of the nucleus should be used in these calculations since the excitation energy is high. The suggestion that the moment of inertia at excitation energies of 20 MeV or more is less than the rigid-body value is unreasonable since pairing forces should be insignificant at these conditions. The initial motivation for the suggestion, namely to obtain the observed low "temperature" when multiple emission has occurred, has been shown to be unnecessary by calculations given in the second section.

We could proceed to determine each single emission spectrum, N_1, N_2, N_3, etc., from the observed total emission spectra N obtained from measurements by the method of the preceding paragraph. For example, consider the observed spectrum for emitted neutrons with energy $E \gtrsim E_m - B_1 - B_2$. This part of the energy spectrum is for a nucleus which emits only one neutron and leaves the residual nucleus in too low an excitation to emit any more neutrons. The energy spectrum where $E_m - B_1 - B_2 \gtrsim E \gtrsim E_m - B_1 - B_2 - B_3$ consists of both first emitted neutrons N_1^{II} (where the superscript denotes the energy region of observed spectra) and second emitted neutrons N_2^{II}. However, if shell-effect differences may be neglected, $N_2^{\mathrm{II}}(E',E)$ may be inferred from N_1^{I}.

$$N_2^{\mathrm{II}}(E',E) = \frac{E}{E'+E+B_2} \times \frac{\sigma_c(E)}{\sigma_c(E'+E+B_2)} N_1^{\mathrm{I}}(E'+E+B_2),$$

where N_1^{I} is the observed energy spectrum in region I where only one neutron could be emitted. We then differentiate the total neutron spectrum in region II with respect to E and obtain

$$\frac{dN^{\mathrm{II}}}{dE} = \frac{dN_1^{\mathrm{II}}}{dE} - N_1^{\mathrm{II}}(E_m - B_1 - B_2 - E) \frac{E}{E_m - B_1} \frac{\sigma_c(E)}{\sigma_c(E_m - E)} N_1^{\mathrm{I}}(E_m - B_1) + \int_0^{E_m - B_1 - B_2 - E} N_1^R(E') \frac{d}{dE}\left[\frac{E}{E'+E+B_2} \frac{\sigma_c(E)}{\sigma_c(E'+E+B_2)} N_1^{\mathrm{I}}(E'+E+B_2) \right] dE'$$

$$\sim \frac{dN_1^{\mathrm{II}}}{dE} + \int_0^{E_m - B_1 - B_2 - E} N_1^R(E') \frac{d}{dE}\left[\frac{E}{E'+E+B_2} \frac{\sigma_c(E)}{\sigma_c(E'+E+B_2)} N_1^{\mathrm{I}}(E'+E+B_2) \right] dE', \quad (25)$$

where $N_1^R(E')$ is the first neutron energy spectrum in the energy range

$$E_m - \sum_{i=1}^{n-1} B_i \gtrsim E' \gtrsim E_m - \sum_{i=1}^{n} B_i,$$

n being the total number of neutrons which can be emitted. Proceeding in this way it would be possible to obtain a system of simultaneous differential equations which would determine N_1 in all the energy regions from the slope of the total neutron distribution curve dN/dE. The experimental uncertainties as well as the theoretical uncertainty due to shell effects are too great to make this method profitable. However, an adaptation of it using Eq. (16) for $\omega(Q)$ may prove profitable.

[25] W. Hauser and H. Feshbach, Phys. Rev. **87**, 366 (1952).
[26] A. M. Lane and K. Parker, Nucl. Phys. **16**, 690 (1960).
[27] T. Erickson and V. Strutinski, Nucl. Phys. **8**, 284 (1958).

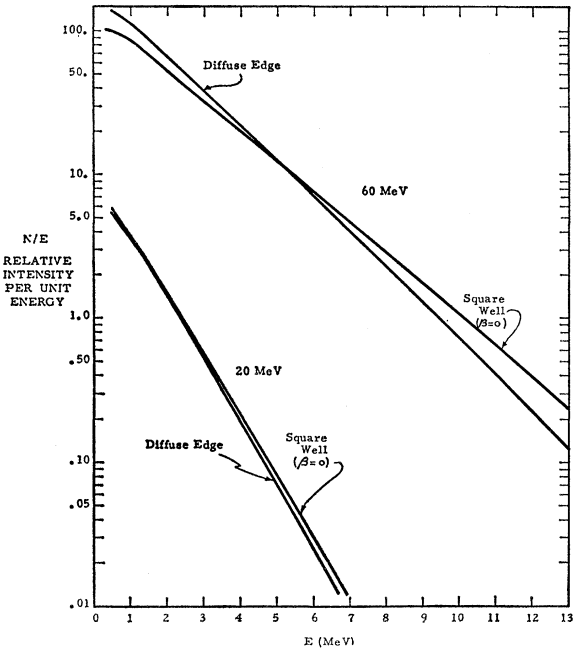

FIG. 8. The effect of using an observed diffuse nuclear potential in place of a square well in the calculated spectrum of the first emitted neutron from a target of Ag^{108} excited to 20 MeV and 60 MeV. $N/E=\exp[2(\alpha Q)^{1/2}+(\beta/3)(Q/\alpha)^{3/2}]$, where $\alpha=10$ MeV^{-1} and $\beta=0.7$ MeV^{-3}.

The results of Sec. III may give us sufficient confidence in the theory that except for the effects of "thermal expansion" we may assume that we already know what the energy spectrum of first emitted neutrons is, namely Eqs. (16), (17), (22), and (23). We anticipate that the primary departure from theory of the experimental data at high excitation energies will occur because of the change in nuclear potential shape as states of high quantum number are occupied. If we represent the "thermal" expansion as an energy dependence of β and expand β in a power series in Q, that is, let

$$\beta=\beta_0+3AQ+3BQ^2, \tag{26}$$

the diffuseness effect factor becomes

$$\exp[(\tfrac{1}{3}\beta_0)(Q/\alpha)^{3/2}]\exp[A(Q/\alpha)^{5/2}+B(Q/\alpha)^{7/2}]. \tag{27}$$

By substituting this expression into Eq. (16) to obtain a better approximation to the nuclear level density and repeating the work of Sec. III, we may determine the values of A and B which best fit the experimental data (including especially charged-particle emission when required since the penetrability is sensitively dependent on the nuclear potential shape[28,29]). The values of A and B may then be interpreted in terms of the energy-dependent change in nuclear potential shape, that is, the energy dependence of η in Eq. (1).

[28] Ken Kikuchi, Progr. Theoret. Phys. (Kyoto) **17**, 643 (1957).
[29] J. M. C. Scott, Phil. Mag. **45**, 441 (1954).

A further complication arises at high excitation in that two kinds of particles may be emitted with roughly equal probability when the excitation energy is high enough to emit protons over the Coulomb barrier with high probability. The transmission of the protons through a diffuse Coulomb barrier[28,29] must be included in the estimate of $\sigma_c(E)$ for protons and the normalization of the neutron emission revised. The fraction of first emitted particles which are neutrons is no longer unity but is given by

$$f_{1n}=\omega_N\int_0^{E_m-B_{1n}}N_{1n}(E_n)dE\Big/\Big(\omega_N\int_0^{E_m-B_{1n}}N_{1n}(E_n)dE+\omega_p\int_0^{E_m-B_{1p}}N_{1p}(E_p)dE\Big), \tag{28}$$

where ω_N is the density of neutron energy levels in the nucleus at zero excitation energy,

$$N_{1n}(E_n)=E_n\sigma_c(E_n)\omega(E_m-B_{1n}-E_n),$$

and the subscript p refers to similar quantities for protons. $f_{1p}, f_{2n}, f_{2p}, \cdots$ are found from similar integrals. $\sigma_c(E_p)$ through a diffuse Coulomb barrier with an unexcited nuclear potential shape is presently being computed and the results of analyzing proton spectra will be reported on later. While neutron spectra at moderate energies may be analyzed neglecting proton emission in those cases for which the reaction energetics do not cause proton emission to be significant, the converse is never true at any excitation energy. The increase in analytical effort required by protons and higher excitation energy is well worthwhile since most proton spectra are obtained with higher resolution than is possible with neutron measurements and the effect of the change in nuclear shape is much more pronounced for protons and higher energies.

V. CONCLUSIONS

The effect of a diffuse nuclear potential on the energy level density and particle evaporation has been found significant at excitation energies of several tens of MeV. The effect of the shape of the nuclear potential on particle-emission spectra increases rapidly with excitation energy and thus particle-emission spectra furnish a tool to determine the shape of the nuclear potential under the unusual and hard to obtain conditions of high nuclear excitation. Even if the nuclear potential shape is independent of excitation energy the diffuseness of the well (determined by elastic neutron scattering) causes the level density to increase as much as two orders of magnitude at 50 MeV excitation energy over that predicted by a square nuclear well shape with noticeable effect on the particle-emission spectra. The expected increase in diffuseness of the nuclear potential at high excitation energy may be observable in the emission spectra and the energy dependence of the shape

of the nuclear potential thereby inferred. By choosing values of r_0 and M consistent with low-energy scattering experiments and our present understanding of nuclear matter a value of α has been derived which yields theoretical nuclear evaporation spectra which fit the present low excitation energy experimental data very well. However, when more precise experimental data at excitation energy ~ 20 MeV become available α may be determined more precisely than is possible at the present time. The dependence of α as well as β on excitation energy may then be interpreted in terms of the properties of nuclear matter ($M^*(E)$ and $\eta(E)$) as higher excitation data become available.

At modest excitation energies of only 14 MeV maximum the effect of the shape of the nuclear potential is relatively unimportant and the theory may be tested by neglecting the expected change in nuclear potential with excitation energy. Neutron emission spectra at modest excitation energy have been computed *without reference to any particle-emission experiments* (that is, nuclear dimensions used in the theory are determined from elastic neutron scattering experiments and the nuclear level densities in a potential of these dimensions are determined entirely theoretically) and the result has been compared successfully to 14-MeV inelastic neutron scattering and (p,n) measurements. Experimental temperature and parameter fitting are not useful concepts when multiple particle emission is at all possible.[19,20] Their experimental determination will result in a possible decrease of "temperature" with excitation energy and a level density parameter an order of magnitude lower than the theoretical value.

ACKNOWLEDGMENTS

We are grateful to John Baker, the computer center on the Davis campus, and the Western Data Processing Center on the Los Angeles campus for help in the machine computing required in Sec. III.

PHYSICAL REVIEW VOLUME 131, NUMBER 6 15 SEPTEMBER 1963

Observable Consequences of Anomalous Thresholds

FRANCIS R. HALPERN AND H. LEE WATSON
University of California, San Diego, La Jolla, California
(Received 2 May 1963)

The Landau surface for the triangle diagram touches the physical region at three points. The consequences of this singlar-matrix element for several processes are studied. It is found that there should be peaks in cross sections at the edge of phase space. These peaks depend sensitively on the incident energy and are distinguished in this way from genuine resonances.

I. INTRODUCTION

THE existence of anomalous thresholds in certain Feynman amplitudes was first noticed by Karplus, Sommerfield, and Wichmann.[1] There has been much subsequent work, particularly by Landau[2] who gave the general conditions for the occurrence of many particle singularities and by Cutkosky[3] who showed how to calculate the discontinuities across their cuts.

In all of the current theoretical approaches to elementary particle physics one abandons many concepts of Lagrangian field theory, but, none the less, assumes that the singularities of the perturbation amplitude are preserved in the correct amplitude.[4,5] Thus, one cannot ignore anomalous thresholds and maintain any semblance of logic. It does not seem a particularly desirable situation, then, that there is no physical evidence that these are anything more than mathematical apparitions.

Landshoff and Trieman[6] and, more recently, Aaron[7] have suggested reactions in which effects of the anomalous threshold occurring in the triangle diagram might be seen. They were limited, however, either by competing diagrams for the same reaction, or by the large distance of the singularity from the physical region. We have found that these limitations can to some extent be removed by allowing two external particles at each vertex of a closed loop graph. Also, we find that under certain conditions, to be described later, the strength of the singularity may be enhanced.

We find that it is necessary to include at least one unstable particle among the internal particles. The imaginary part of the mass of this particle keeps the singularity from actually touching the boundary of the physical region. For a narrow resonance this might not be too serious. In fact, if the effect turns out to be observable, it might provide some information on the widths of such resonances.

[1] R. Karplus, C. M. Sommerfield, and E. H. Wickmann, Phys. Rev. **111**, 1187 (1958).
[2] L. Landau, Nucl. Phys. **13**, 181 (1959).
[3] R. E. Cutkosky, J. Math. Phys. **1**, 429 (1960).
[4] H. Stapp, Phys. Rev. **125**, 2139 (1962).
[5] G. Kallen and A. S. Wightman, Kgl. Danske Videnskab. Selskab, Mat. Fys. Medd. **1**. 6 (1958).
[6] P. Landshoff and S. B. Treiman, Phys. Rev. **127**, 649 (1962).
[7] R. Aaron, Phys. Rev. Letters **10**, 32 (1963).